The Challenge of Ambient Air–Processed Organometallic Halide Perovskite: Technology Transfer From Spin Coating to Meniscus Blade Coating of Perovskite Thin Films

Patrick Wai-Keung Fong* and Gang Li*

Department of Electronic and Information Engineering, Research Institute for Smart Energy (RISE), The Hong Kong Polytechnic University, Hong Kong

The development of perovskite solar cells (PSCs) has been extensively studied in the past decade, and the power conversion efficiency (PCE) has reached a record of 25.2%. Despite impressively high PCE, the fabrication process mainly relied on a well-controlled environment, an inert gas–filled glovebox, and devices of small areas were demonstrated. This impedes the technology transfer from laboratory scale spin coating to manufacturing ambient air scalable processes. Furthermore, the nucleation and crystal growth processes of the perovskite thin films are different when the films are prepared in different environmental conditions. In this review, we summarize the recent advances of ambient air–processed organometallic halide perovskite thin films. Focuses are made on the impact of ambient air conditions, typically adventitious moisture, on the crystallization of perovskites thin films. The challenges and strategies in the technology transfer from the glovebox or ambient air spin coating to scalable meniscus blade coating are also discussed to shed light on the manufacture of ambient air–processed PSCs.

Keywords: ambient fabrication, spin coating, meniscus blade coating, perovskite solar cells, scalable large area, nucleation, supersaturation, air-knife

INTRODUCTION

Organic–inorganic hybrid perovskite solar cells have received tremendous attention in the photovoltaic field of study in the past decade because the active perovskite layer exhibits excellent optoelectronic and intrinsic properties such as high carrier mobility, long charge carrier diffusion length ($\sim$100 μm), large optical absorption coefficient ($\sim$$10^5$ cm^{-1}), low exciton binding energy ($\sim$20 meV), and low nonradiative recombination losses (Liu et al., 2013; Correa-Baena et al., 2017); flexible bandgap tunability (Noh et al., 2013; Saliba et al., 2016); and ease of low-temperature solution process facilitating low-cost fabrication of photovoltaic devices (Dunlap-Shohl et al., 2019). Perovskite has a chemical formula of AMX_3, where the monovalent organic cation A is the organic cation occupying the 12-fold coordinated holes within the cavity, M is the metallic cation, and X is the halogen anion forming the octahedral structure. Typically, methylammonium (MA$^+$), formamidinium (FA$^+$), and cesium (Cs$^+$) are the mostly used A-site organic cations; Pb^{2+} and Sn^{2+} are the metallic divalent cations, and I$^-$, Br$^-$, and Cl$^-$ are the halogen anions. There is a remarkable progress of the perovskite solar cells (PSCs) in the past decade in which the record power conversion

efficiency (PCE) of organic–inorganic hybrid perovskite solar cells (PSCs) has increased rapidly from its debut of 3.8% (Kojima et al., 2009) to the latest certified record of 25.2% (NREL, 2020). The perovskite material was first used as sensitizers for the liquid electrolyte in dye-sensitized solar cells by Miyasaka in 2009, and the reported PCE was 3.8% (Kojima et al., 2009). However, the so-called *perovskite fever* appeared since the solid-state organic–inorganic hybrid perovskite solar cell was reported by Park et al. and Snaith et al. with a PCE of ~10% in 2012 (Kim et al., 2012; Lee et al., 2012). The breakthrough was not only the efficiency improvement but also the stability of the device by avoiding the use of the liquid electrolyte. Since then, huge efforts were made on the strategies to improve the crystallization and nucleation of the perovskite thin films and the perovskite film morphology.

The state-of-the-art PSCs are typically fabricated in a well-controlled environment such as an inert gas–filled glovebox. While the best performing laboratory PSC exhibits a record PCE of 25.2% (NREL, 2020) which is approaching the theoretical limit based on the Shockley–Queisser (S-Q) theory, the PCE of the PSCs prepared in ambient air still lags behind those processed in the inert gas–filled glovebox. Researchers start to explore the technology transfer of the PSC fabrication process from the laboratory to manufacturing by different approaches mostly focused on the strategies avoiding the influence of adventitious moisture on the perovskite thin film nucleation and crystallization. Liu et al. adopted 4-*tert*-butylpyridine (tBP) as an additive to the precursor solution to increase the moisture resistance attributed to the hydrophobic property of the additive (Liu et al., 2017). Troughton et al. used anti-solvent of higher water solubility, ethyl acetate, for the crystallization protocol to extract moisture from the intermediate phase of the perovskite layer (Troughton et al., 2017). Toward industrial fabrication of PSCs, ambient air processing and scalability are two important issues to be explored systematically. It is known that the crystallinity and surface morphology of the perovskite material are very sensitive to the ambient conditions, especially the airborne moisture. However, encouraging results by moisture-induced crystallization have been reported in PSCs by different groups (You et al., 2014; Zhou et al., 2014; Rong et al., 2017).
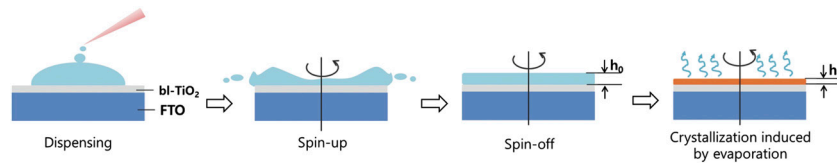
In this review, we summarize the progress of PSCs toward upscaling fabrication by in-depth discussion of the crystallization process of both spin-coating and roll-to-roll–compatible blade-coating methods. First, the progress of the development of PSCs will be explored. The fabrication processes from the laboratory-scaled spin-coating method to the industrial roll-to-roll–compatible blade-coating method are discussed in detail based on the differences in drying kinetics and processing window between these two coating methods. Second, the advances of ambient air–processed PSCs are summarized including the strategies avoiding moisture attack during the crystallization process, the methodologies improving crystallinity, and the challenges and pathways toward the manufacturing-compatible fabrication process—scalability. Finally, we provide an outlook on the challenges associated with the environmental and manufacturing issues.

PROGRESS OF PSCS: TOWARD UPSCALING FABRICATION

There has been a steady improvement in the development of highly efficient PSCs in the past decade, and the record certified efficiency is 25.2% (NREL, 2020). However, most of the highly efficient devices were prepared by the spin-coating method. Facile spin-coating solution process technique is very useful in the laboratory research scale, but the drawbacks are the wastage of chemical solution, most of the drop casted solution being wasted in the spin-coating process, and the limitation of the substrate size to maintain spun film uniformity and quality. Although modules of size 100 cm^2 were fabricated by the spin-coating method (Seo et al., 2014), the PCE was considerably reduced as the size of the device was increased. For mass production, scalability is one of the major factors that researchers need to consider in the early stage of research. The technology transfer from the laboratory scale to the manufacturing scale is limited especially in perovskite solar cells, in which the film formation involves different stages of the chemical reaction. In addition, the manufacture of perovskite solar cells faces another challenge, besides scalability, which is the impact of airborne moisture on the perovskite film formation and morphology. It is well known that the device performance of the PSC is significantly affected by the grain size and the morphology of the perovskite thin film. In the following sections, we first discuss the scalability issue and then the strategies in the fabrication of perovskite solar cells in ambient conditions. The state-of-the-art PSCs are fabricated by facile spin-coating solution process technique, but it is incompatible with mass production. Toward the manufacturing process, upscaling technique should be implemented in the early research stage. Scalable solution processes for the fabrication of PSCs include slot-die coating (Hwang et al., 2015; Qin et al., 2017; Galagan et al., 2018), spray coating (Heo et al., 2016; Tait et al., 2016), inkjet printing (Li et al., 2015), screen printing (Mei et al., 2014; Rong et al., 2017), electrodeposition (Cui et al., 2015; Huang et al., 2015), and meniscus blade coating. Among these scalable deposition methods, the blade-coating method received more awareness in the development of upscaling of perovskite solar cells because it is compatible with roll-to-roll fabrication. In this review, we focus on the discussion of the development of scalable deposition of PSCs using the meniscus blade–coating method.

Scalable Meniscus Blade Coating of Perovskite Thin Films

Meniscus blade coating is a facile and roll-to-roll–compatible deposition method in which a small amount of precursor solution is injected, by the capillary force, into the gap between the blade and the substrate to form a static wet line. Then, the blade (or the substrate) is moved laterally to coat a layer of the precursor wet film on the substrate. Several parameters are taken into consideration for the film formation process: the spacing between the substrate and the blade, amount of applied solution, linear coating speed, viscosity (dependent on the

FIGURE 1 | Illustrations of the dynamic evaporation of solvent in the spin-coating process. Reprinted with permission from Heo et al. (2014). Copyright 2014 WILEY-VCH Verlag GmbH & Co. KGaA, Weinheim.

concentration or solvent used) of the precursor solution, and wettability of the precursor solution on the substrate (Le Berre et al., 2009). In addition, the drying kinetics (evaporation rate of the solvent) is also a crucial parameter in the blade-coating process, which significantly affects the processing window, perovskite thin film morphology, crystal grain size, and final photovoltaic device performance (Hu et al., 2019). This can be controlled by different strategies including solvent engineering (Yang et al., 2017), hot substrate at the blade-coating step (He et al., 2017; Wu et al., 2018), and gas-assisted drying (gas quenching) (Ding et al., 2019; Hu et al., 2019; Liu et al., 2020).

Intrinsic Difference in Drying Mechanisms Between Spin-Coating and Blade-Coating Methods

The film formation process of the spin-coating deposition method cannot be transferred directly to that of the blade-coating deposition method. There are structural differences in solvates prepared by spin-coating and blade-coating techniques (Zhong et al., 2018). It is not difficult to expect that the evaporation rate of the solvent for a dynamic (spin-coating) sample is different from that for a static (blade-coating) sample. In the spin-coating deposition process, excess solution is spun off the substrate to produce a uniform wet film of thickness h_0, as shown in **Figure 1** (Heo et al., 2014). The continuous spinning induces further evaporation of solvent and thinning of the wet film. The wet film thickness, h, as a function of spinning time can be expressed as (Lawrence, 1988; van Hardeveld et al., 1995; Heo et al., 2014)

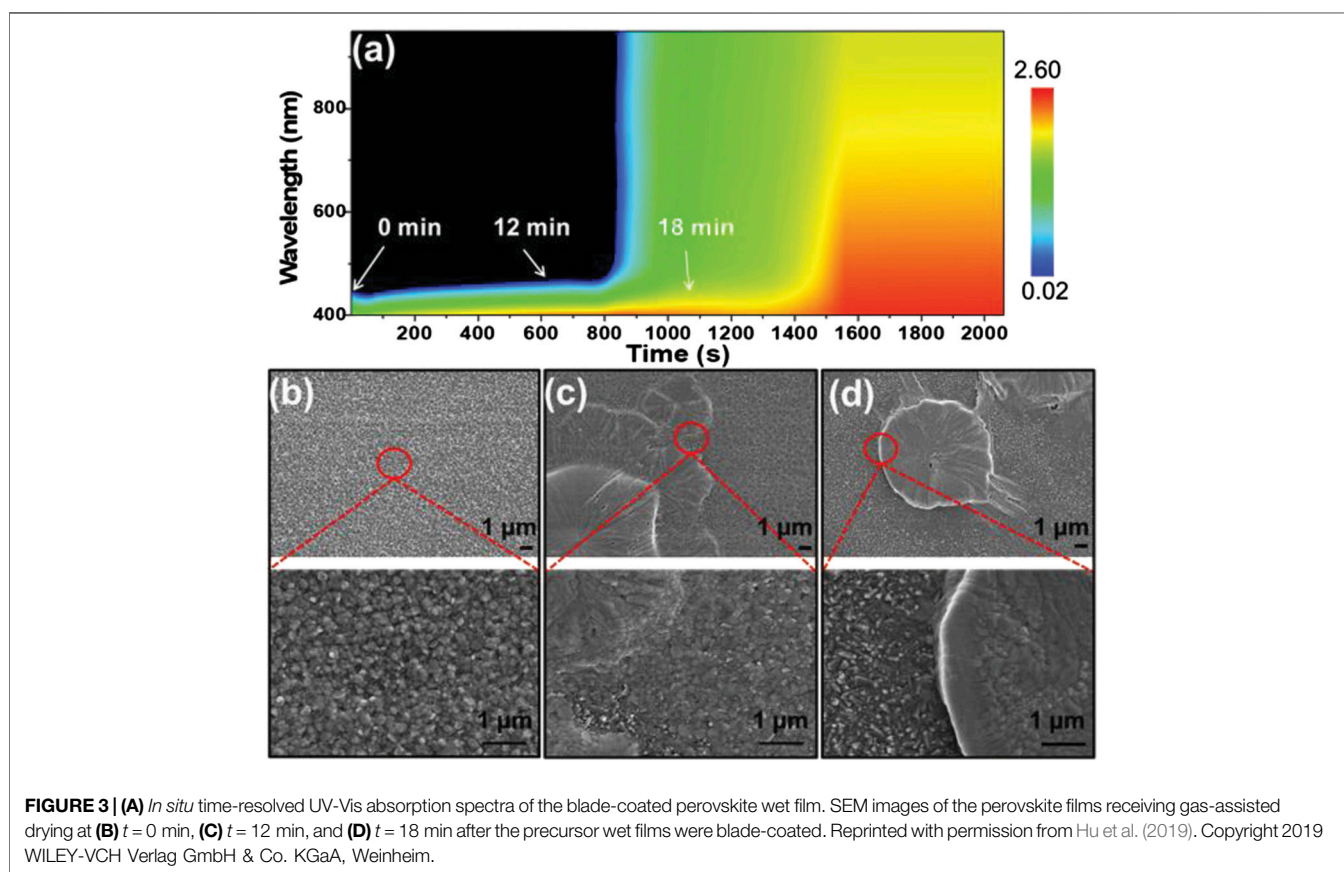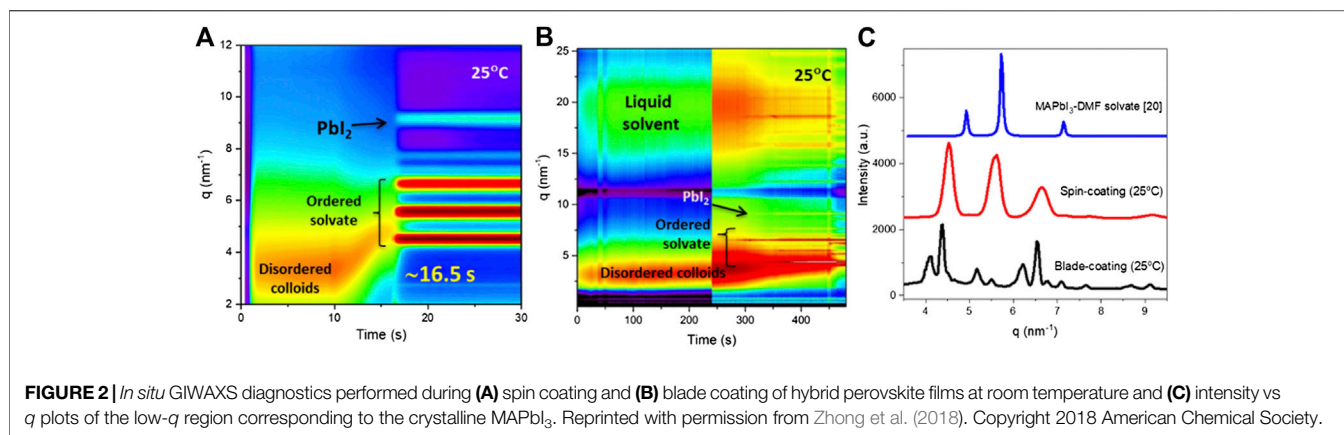$$\frac{dh}{dt} = -\frac{2\rho\omega^2}{3\eta}h^3 - \phi, \tag{1}$$

where ω is the radial velocity, ϕ is the evaporation rate induced by spinning, and ρ and η are the density and viscosity of the solution, respectively. The evaporation of solvent results in an increase in the concentration of the solute, and if it reaches the concentration of supersaturation, nucleation is initiated (Hu et al., 2020). The final film thickness, h_f, is dependent on the solidification process of the perovskite material.

For the blade-coating process, the evaporation rate of the solvent is very different from that during a spin coating–induced evaporation. Thus, the well-developed deposition recipe using the spin-coating method requires appropriate modification for the implementation in the blade-coating method. Detailed studies are

needed to gain the insight into the optimization of the fabrication recipe. Zhong et al. performed an *in situ* GIWAXS investigation on the ink-to-solid solidification process for the two different coating methods (**Figure 2A–C**) (Zhong et al., 2018). It was found that the blade-coated wet film took longer time to dry than the spin-coated wet film, exhibiting highly disordered solvates (blade-coated film) vs crystalline solvates (spin-coated film). The relatively low evaporation rate of the solvent in the blade-coated wet film facilities the growth of larger grain size, but this is difficult to form a compact and pinhole-free film when dried naturally (Kim et al., 2015). Different strategies were adopted to create rapid solvent extraction, resulting in the supersaturation of the solution, such as hot-substrate casting (He et al., 2017; Wu et al., 2018) and gas-assisted drying (Ding et al., 2019; Hu et al., 2019; Liu et al., 2020).

The Processing Window of Spin Coating and Blade Coating of Perovskite Thin Films

Highly efficient PSCs fabricated by the spin-coating method typically rely on the application of anti-solvent to extract the solvent from the precursor solution rapidly. Rapid supersaturation of the precursor solution is achieved to initiate the formation of crystal nuclei (Thanh et al., 2014). However, anti-solvent is not technically compatible with the blade-coating method, and its toxicity is not ambient environment friendly. The control of supersaturation has a significant impact on the nucleation rate, the grain size, and subsequently the final film morphology. In the spin-coating method, it is known that the process window, the precise control of time to drop cast the anti-solvent, and the duration of the drop cast process for the application of anti-solvent are very narrow. It is not the favor process for roll-to-roll manufacturing, and the reproducibility is also significantly affected. This would be a big challenge especially when the manufacturing process takes place in ambient conditions. There are other strategies to create the supersaturation state of the precursor solution such as gas quenching, hot-substrate drop casting, and vacuum-assisted drying, in which the first two drying techniques are widely studied. Hu et al. studied the process window of the blade coating of mixed halide perovskite solar cells (Hu et al., 2019). A laminar air-knife–assisted blade-coating technique was adopted, enabling the *in situ* study of the drying kinetics of the perovskite film by time-resolved UV-Vis spectroscopy. A wide process window, up to 12 min, enabled the fabrication of highly efficient meniscus blade–coated PSCs performed in an
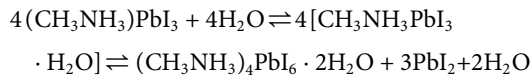
FIGURE 2 | *In situ* GIWAXS diagnostics performed during **(A)** spin coating and **(B)** blade coating of hybrid perovskite films at room temperature and **(C)** intensity vs *q* plots of the low-*q* region corresponding to the crystalline MAPbI₃. Reprinted with permission from Zhong et al. (2018). Copyright 2018 American Chemical Society.

FIGURE 3 | **(A)** *In situ* time-resolved UV-Vis absorption spectra of the blade-coated perovskite wet film. SEM images of the perovskite films receiving gas-assisted drying at **(B)** *t* = 0 min, **(C)** *t* = 12 min, and **(D)** *t* = 18 min after the precursor wet films were blade-coated. Reprinted with permission from Hu et al. (2019). Copyright 2019 WILEY-VCH Verlag GmbH & Co. KGaA, Weinheim.

inert gas–filled glovebox (**Figure 3A**). The rapid change in absorption of the blade-coated precursor wet film by gas quenching, analogous to anti-solvent in spin-coating technique, can also be recorded, providing insights into the drying kinetics, degree of supersaturation, crystal nucleation and growth, and final film morphology (**Figure 3B–D**). Yang et al. reported that the process window could be extended from several seconds to several minutes by using different solvent compositions, attributed to the different evaporation rates of solvents (Yang et al., 2017).

DEVELOPMENT OF AMBIENT AIR–PROCESSED PSCS—TOWARD MANUFACTURE

Perovskite thin films undergo severe degradation in the presence of oxygen and moisture, and high-quality perovskite films are typically prepared in inert gas–filled gloveboxes. Because of the chemical complexity of the precursor solution, the presence of oxygen and moisture in ambient air results in an uncertainty of the precursor recipe developed for the glovebox process to be

transferred to the ambient process. Water molecules *attack* the perovskite film by forming the $(CH_3NH_3)_4PbI_6$ di-hydrated phase and PbI_2 via the chemical reaction (Radicchi et al., 2020)

$$4\,(CH_3NH_3)PbI_3 + 4H_2O \rightleftharpoons 4\,[CH_3NH_3PbI_3$$

$$\cdot\, H_2O]\rightleftharpoons (CH_3NH_3)_4PbI_6 \cdot 2H_2O + 3PbI_2 + 2H_2O$$

The mono-hydrated phase is reversible when receiving subsequent dry treatment (Leguy et al., 2015). This stage is reported as a beneficial factor which helps to enhance the crystallization process to increase the grain size and achieve better crystallinity. The improved lattice crystallinity induces enhanced photovoltaic performance (Heo et al., 2014; Gong et al., 2015; Wu et al., 2015; Chiang et al., 2017) and the stability (Contreras-Bernal et al., 2018) of the PSCs. When the chemical reaction proceeds further to the right with prolonged exposure to water molecules, a di-hydrated phase is formed accomplished by two water molecules. The release of two water molecules provides the self-sustainability of the chemical reaction process, resulting in the degradation of the complete perovskite film. Computational studies also showed that aqueous solutions inhabited the formation process of perovskites, but small amount of water could be added as an additive for the deposition of perovskite materials (Radicchi et al., 2020). A study has been conducted recently to provide a comprehensive understanding of the improvement of PSC stability against water molecules through compositional engineering (Li et al., 2021). Initial studies have been conducted on the synthesis of water-stable perovskites for the application of light-emitting devices (Jana and Kim, 2018; Ba et al., 2019). In the following section, we will discuss the impact of airborne moisture on the ambient air–processed perovskite thin films and summarize the advances of upscaling fabrication of perovskite materials in the ambient environment.

Impact of Airborne Moisture

Airborne moisture attack is the most challenging technical issue to face to successfully transfer the perovskite solar cell fabrication process from the well-controlled environment (inert gas–filled glovebox) to the ambient conditions. It is known that, for a fabricated perovskite device (film formation process is completed), the organic components would be attacked by moisture and the perovskite active layer would be decomposed, and hence, both the device performance and stability were significantly affected. However, the influence of the presence of moisture during the fabrication process (nucleation and crystal growth) on the perovskite crystallinity is unclear. There were some contradictory results when the perovskite layers were prepared in an ambient environment with intrinsic or extrinsic moisture content. Zhou et al. reported that the moisture level at RH = 30% resulted in an enhanced reconstruction in film formation by partially dissolving the reactant species and accelerating mass transport in the film. This humidity enhanced reconstruction strategy improved the PCE from 13.5% (control) to 16.4% for the device of architecture ITO/TiO$_2$/pvsk/spiro-OMeTAD/Au (Zhou et al., 2014). Although excess moisture could damage the crystal structure

of perovskites, You et al. reported a similar positive effect of a small amount of moisture in the annealing stage of the film formation process could improve the film crystallinity (grain size), carrier mobility, and lifetime of p–i–n devices, with the PCE boosted from 12.3% to 15.4% (You et al., 2014). Pathak et al. studied the effect of annealing parameters (annealing atmosphere, time, and temperature) on the crystallinity of the perovskite thin film. They also found that annealing in air resulted in better crystallinity and a larger grain size than annealing in nitrogen ambient (Pathak et al., 2015). Although moisture (with proper moisture level) could be an advantage for the annealing stage, it has been reported that moisture should be avoided during the spin coating–induced nucleation stage (Gao et al., 2015). It is also interesting to note that the aqueous HI (57 wt% in H$_2$O) additive in the MAPbI$_3$ one-step spin-coating process can significantly improve the device performance, attributed to the prevention of decomposition of MAPbI$_3$ into MAI and PbI$_2$ (Heo et al., 2015a; Heo et al., 2015b). However, the water content in HI solution does not have any apparent adverse effect on the thin film crystallinity. A similar observation was reported by Heo et al. (2014) that devices fabricated by the precursor solution prepared by DMF + H$_2$O or DMF + HBr(aq.) were better than those prepared by pure DMF because the addition of H$_2$O or aqueous HBr exhibited better solubility than pure DMF. In general, it is a competing process between the nucleation in the spin-coating stage and the film-annealing stage in ambient conditions. Relatively dry ambient favors the supersaturation in the spin-coating stage, resulting in high nucleation densities for the formation of a compact and smooth thin film. In the annealing stage, proper moisture content is beneficial to the formation of perovskite films with good crystallinity, which is attributed to the modest supersaturation (You et al., 2014; Gao et al., 2015; Pathak et al., 2015). Thus, control of supersaturation has proven to be the crucial factor to control the nucleation and hence the final film grain size and morphology. In ambient conditions, airborne moisture could "dilute" the solute, impeding the supersaturation of the precursor wet film.

As discussed above, the impact of airborne moisture could be an advantage or disadvantage to the solidification process of the perovskite thin film. To gain more insights into the effect of kinetics of the moisture on the film formation in ambient conditions, researchers performed systematic studies by intentionally (extrinsically) adding water content in the fabrication of the perovskite thin film. Wu et al. performed a systematic study on the water additive, varied from 0 to 4 wt% to DMF, in PbI$_2$+DMF solution using a two-step deposition method for the inverted device structure, and the best device was produced from the solution with 2 wt% H$_2$O additives (with better surface morphology and film coverage) (Wu et al., 2015). Although the PCE with optimized water content could produce a device of PCE 18%, the mechanisms for the water enhanced morphology were unclear. Gong et al. (2015) also used a similar water additive method in the one-step deposition method for CH$_3$NH$_3$PbI$_{3-x}$Cl$_x$, whereas Heo et al. (2014) used a water additive method in the one-step deposition method for MAPbBr$_3$. Both reported better devices were achieved with a
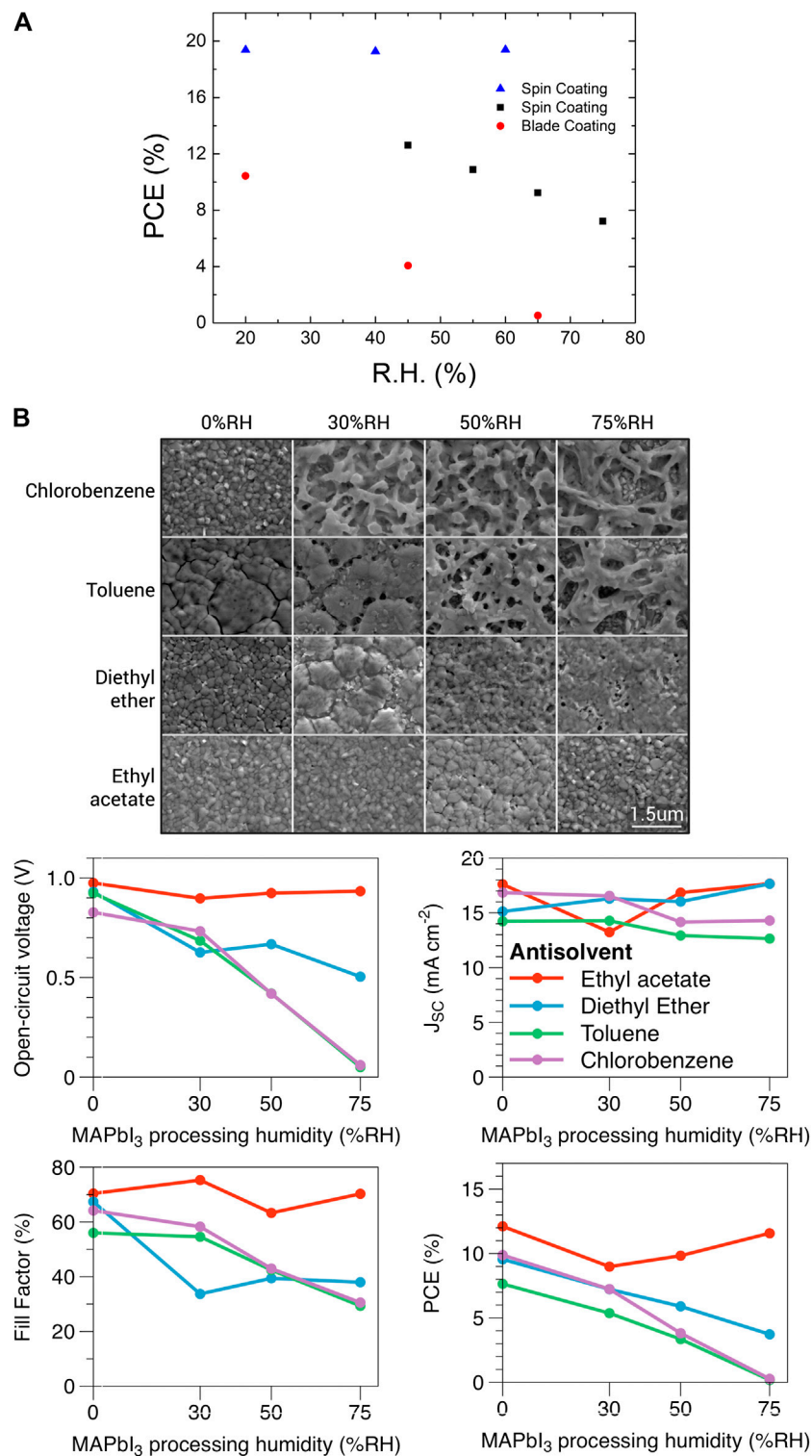
FIGURE 4 | (A) Photovoltaic performance of the perovskite thin films fabricated in ambient conditions at different relative humidity levels. Data are extracted from (Liu et al., 2017) for the two-step spin-coating method (squares), (Yang et al., 2015) for the blade-coating method (circles), and (Cheng et al., 2019) for the two-step spin-coating method with an optimized molar ratio at specific RH (triangles). **(B)** SEM micrographs of the perovskite films fabricated by the spin-coating method at different RH levels and different anti-solvents and the corresponding photovoltaic device parameters. Adapted under the terms of the CC-BY Creative Commons Attribution 4.0 International License (http://creativecommons.org/licenses/BY/4.0/) (Troughton et al., 2017). Copyright 2017 The Authors. Published by Elsevier Ltd.

TABLE 1 | Strategies to control the nucleation and growth of perovskite films fabricated in ambient conditions.

Perovskite composition	Methodology	Ref.
MAPbI$_3$ (one-step)	tBP additive (hydrophobic) to increase the moisture resistance	Liu et al. (2017)
MAPbI$_3$ (one-step)	Anti-solvent of higher water solubility to extract moisture from intermediate phase	Troughton et al. (2017)
MAPbI$_3$ (one-step)	NH$_4$Cl additive and moisture–assisted crystallization	Rong et al. (2017)
MAPbI$_3$ (two-step)	Optimized molar ratio for different ambient RH levels	Cheng et al. (2019)
MAPbI$_3$ (two-step)	ZnO nanoparticle–induced crystallization	Wang et al. (2018)
MAPbI$_3$ (two-step)	Hot substrate	Cheng et al. (2017)
MAPbI$_3$ (two-step)	Hot substrate	Ko et al. (2015)
MAPbI$_{3-x}$ (SCN)$_x$ (two-step)	Lead(II) thiocyanate precursor	Tai et al. (2016)
Cs$_x$ (FA$_{0.83}$MA$_{0.17}$) $_{(1-x)}$Pb(I$_{0.83}$Br$_{0.17}$)$_3$	Cs-controlled grain growth at low RH (15–25%)	Singh and Miyasaka (2018)

proper amount of water additive than with anhydrous precursor solution. Therefore, a suitable amount of water is beneficial to promoting the grain growth, but excess amount of water is detrimental because it dilutes the precursor concentration, affecting the supersaturation condition.

Strategies to Deposit Compact Perovskite Film in Ambient Conditions

Typically, PSCs fabricated in ambient conditions of high relative humidity exhibit a poor photovoltaic performance, as shown in **Figure 4A**. The decrease in PCE is attributed to the poor film coverage and nucleation of the perovskite thin film which is attributed to the impeding supersaturation of the precursor wet film by moisture dilution. Troughton et al. (2017) performed systematic studies on the preparation of the perovskite layer in ambient conditions at different humidity levels (**Figures 4B**). As expected, the higher the relative humidity (RH), the poorer the film coverage (providing a shunt path of the device). Their studies also found that anti-solvent with higher water solubility (as both anti-solvent and water absorber) produced better film coverage at high humidity levels. Ethyl acetate, an anti-solvent with higher water solubility, could minimize the moisture exposure of the intermediate phase MAI-PbI$_2$-DMSO, which is known to be very unstable in moisture (Jung et al., 2014). Cheng et al. (2019) optimized the molar ratio of the precursor solution targeted for the fabrication of PSCs at different RH levels (from 20% to 60% RH) to maintain a constant PCE (**Figure 4A**). Similar results have been reported by Aranda et al. to optimize the DMSO:Pb ratio of the perovskite ink targeted at different RH levels (Aranda et al., 2017). Although the PCE is independent of the ambient RH (ranging from 20 to 60%), the processing window is very narrow especially when there is a day-to-day variation in RH. There are also different strategies to minimize the impact of high humidity conditions on the spin-coating deposition of the perovskite thin film in ambient conditions. tBP was used as an additive for one-step deposition of MAPbI$_3$, which is beneficial to its hydrophobic property to increase the moisture resistance in the solidification process (Liu et al., 2017). The Han group used NH$_4$Cl as an additive to improve the grain size and film morphology via moisture-assisted nucleation (Rong et al., 2017). There are also some other strategies to control the nucleation in the ambient conditions summarized in **Table 1** (Ko et al., 2015; Tai et al., 2016;

Cheng et al., 2017; Liu et al., 2017; Rong et al., 2017; Troughton et al., 2017; Singh and Miyasaka, 2018; Wang et al., 2018; Cheng et al., 2019). However, the use of anti-solvent is very ineffective for large scale device production, and the reproducibility is not desired because of the complex dynamics. In the next section, we will discuss the upscaling fabrication of PSCs in the ambient environment by the meniscus blade–coating method.

Ambient Blade Coating–Processed PSCs—Keys to Success

Yang et al. performed the blade coating of perovskite layer in ambient conditions at different relative humidity levels, varying from 15% to 70% (Yang et al., 2015). Their findings suggested that the airborne moisture significantly affected the nucleation and crystal growth of perovskites, as shown in **Figure 5A–F**. As expected, the corresponding PCE of the PSCs decreased as the fabrication ambient RH increased. A PCE of 10.71% was obtained for the device fabricated at RH = 15–25%, whereas the reference device fabricated in a glovebox with H$_2$O < 0.1 ppm showed a comparable PCE of 11.32%. This evidence shows that airborne moisture affects the perovskite nucleation and growth mechanisms although it is still processable at RH < 25% (a limiting factor in manufacturing). In this section, we will explore different strategies to form a compact and high-quality perovskite film under ambient conditions: hot-substrate coating, compositional engineering, adding additives, solvent engineering, adding surfactant, and gas quenching.

The film formation process for the meniscus blade–coating method is different from that of the spin-coating method (Kim et al., 2015). As discussed in the previous sections, the process transfer from spin coating to blade coating is not straightforward due to the complexity of the chemical process (Yang et al., 2017) and also the different solvent evaporation rates during the spinning and blading stages, as shown in **Figure 2A,B** (*in situ* GIWAXS) (Zhong et al., 2018). It was found that the evaporation rate of the solvent could be accelerated by heating the substrate when the blade coating of wet film was conducted (Deng et al., 2015; Kim et al., 2015; Zhong et al., 2018). The hot substrate provides thermal energy to evaporate the solvent to approach the supersaturation to initiate the nucleation process. It is worthy to note that the intermediate phase is very sensitive to moisture. Thus, blade coating on the hot substrate, with optimized

TABLE 2 | Comparison of some representative PSCs with perovskite thin films fabricated by the blade-coating method in the ambient environment.
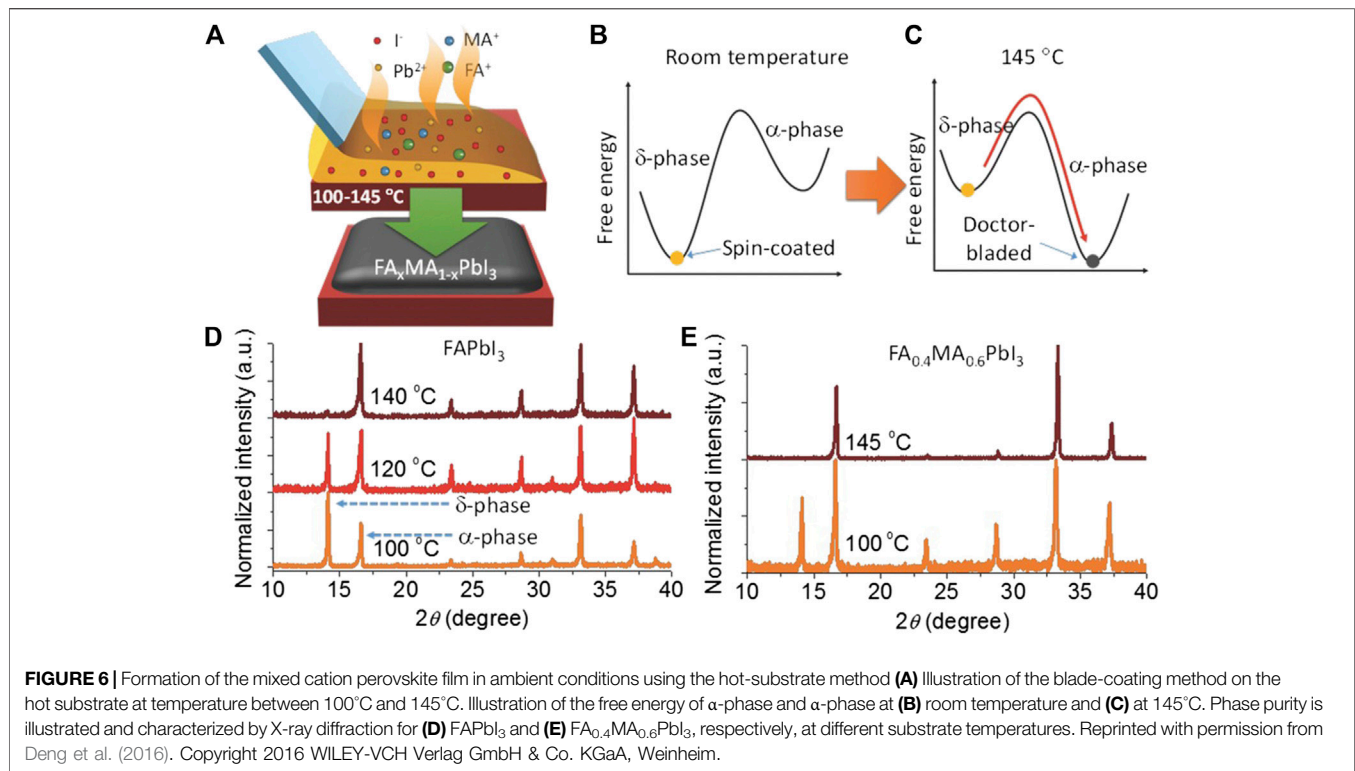
Perovskite composition	Crystallization protocol	RH (%)	PCE (%)	Ref.
$MAPbI_xCl_{3-x}$	Hot substrate (60°C)	15–25%	10.71%	Yang et al. (2015)
$MAPbI_xCl_{3-x}$	Hot substrate (60°C)	40–50%	4.07%	Yang et al. (2015)
$MAPbI_xCl_{3-x}$	Hot substrate (60°C)	60–70%	0.53%	Yang et al. (2015)
$MAPbI_3$	Hot substrate (150°C)	25–45%	7.32%	Mallajosyula et al. (2016)
$MAPbI_3$	NH_4Cl additive; gas quenching	30–50%	19.72%	Dai et al. (2020)
$FA_{0.85}MA_{0.15}PbI_{2.55}Br_{0.45}$	Hot substrate (60°C)	30%	20.05%	He et al. (2017)
$CsPbI_2Br$	Hot substrate (80°C)	35%	14.7%	Fan et al. (2019)
$Cs_{0.05}FA_{0.8}MA_{0.15}PbI_{2.55}Br_{0.45}$	Hot substrate (150°C)	50%	18.2%	Tang et al. (2020)
$FA_{0.85}MA_{0.15}PbI_{2.55}Br_{0.45}$	Hot substrate (150°C)	50%	15.8%	Tang et al. (2020)
$Cs_{0.05}FA_{0.8}MA_{0.15}PbI_3$	Hot substrate (150°C)	50%	16.3%	Tang et al. (2020)
$FAPbI_{2.55}Br_{0.45}$	Hot substrate (150°C)	50%	13.9%	Tang et al. (2020)
$FAPbI_3$	Hot substrate (150°C)	50%	12.35%	Tang et al. (2020)
$MAPbI_3$	Hot substrate (150°C)	55%	17.5%	Zhong et al. (2018)
$MAPbI_3$	Hot substrate (145°C); L-α-phosphatidylcholine additive	Not specified	20.3%	Deng et al. (2018)
$MAPbI_3$	Hot substrate (85°C); gas quenching	Not specified	19.5%	Ternes et al. (2019)
$MAPbI_3$	Gas quenching with mixed solvent (DMSO, DMF, ACN, 2-ME)	Not specified	21.3%	Deng et al. (2019)
$MAPbI_3$	Diethyl ether bath; MACl additive	10–20%	19.05%	Yang et al. (2017)
$MAPbI_3$	Hot substrate (150°C); "non-toxic" solvent	45%	18.0%	Bi et al. (2018)
$Cs_{0.05}FA_{0.8}MA_{0.15}PbI_{2.55}Br_{0.45}$	Gas quenching	55%	21.1%	Fong et al. (2021)
$MAPbI_3$	Hot substrate (150°C); "non-toxic" solvent	Not specified	17.02	Huang et al. (2020)
$MAPbI_3$	Hot substrate (135°C); $PbAc_2 \cdot 3H_2O$ lead source	45%	16.4%	Kong et al. (2018)
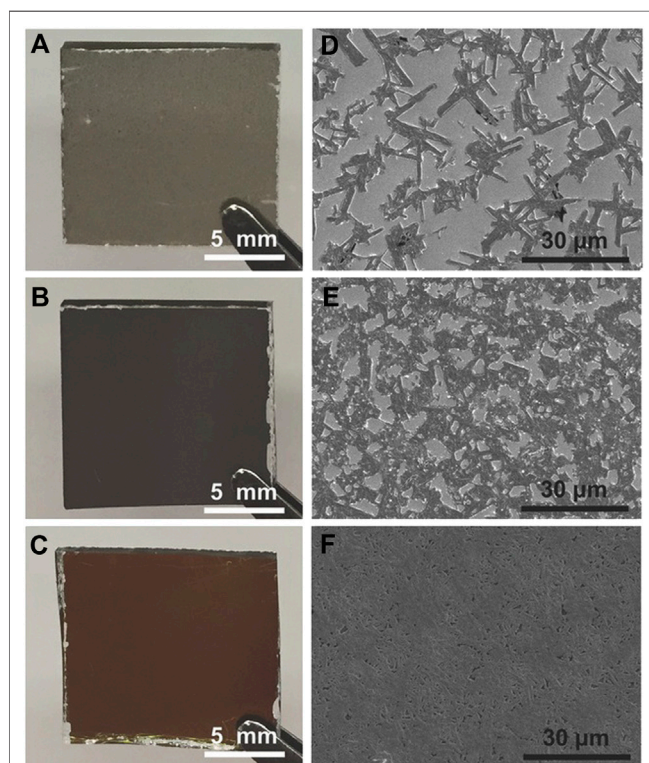
FIGURE 5 | Photographs and SEM micrographs of the perovskite thin films fabricated by blade-coating technique at different RH levels. Images were taken at **(A, D)** RH = 50–70%, **(B, E)** RH = 40–50%, and **(C, F)** RH = 15–25%. A compact perovskite film was obtained under RH = 15–25%, and needle-like crystallites were observed for the sample fabricated under RH = 60–70%. Reprinted with permission from Yang et al. (2015). Copyright 2015 WILEY-VCH Verlag GmbH & Co. KGaA, Weinheim.

temperature, can accelerate the solidification process from the wet film via the intermediate phase to the final solid state to minimizing the intermediate phase being attacked by moisture. *In situ* GIWAXS was conducted, and no intermediate solvates were observed at substrate temperature >100°C. A PCE of 17.5% was achieved at a substrate temperature of 150°C. The drawback of the high-temperature process is the difficulty in blade coating on flexible substrates.

Compositional engineering is another key aspect to be considered in the ambient air–processed perovskite solar cells. $MAPbI_3$ is widely used as the active layer in PSCs. However, its bandgap energy is too large for achieving maximum efficiency. The alloying of mixed cations (FA and MA) can tune (reduce) the bandgap energy, thereby increasing the short-circuit current which is attributed to the broadening of the solar absorption spectrum. However, pure FA-based perovskite materials suffer from poor phase stability and high moisture sensitivity. Deng et al. tuned the composition of the perovskite ($FA_{0.4}MA_{0.6}PbI_3$) to extend the absorption onset to 850 nm (Deng et al., 2016). The perovskite layer was prepared by doctor blade coating on the hot substrate at 140°C to form the α-phase (**Figure 6A–E**), and a device PCE of 18.3% was demonstrated. The same group then further optimized the ink formulation by adding a small fraction of Cs cations and Br anions to lower the process substrate temperature to 120°C in the blade-coating process of the $Cs_{0.02}FA_{0.38}MA_{0.6}PbI_{2.975}Br_{0.025}$ perovskite film (Tang et al., 2017). However, the devices fabricated under these conditions shunt easily. MACl was used as an additive to slow down the grain growth in the film-annealing stage, thereby forming a smoother and more compact film and reducing the shunt pathway of the device (Dong et al., 2015; Tang et al., 2017). A PCE of 19.3% was demonstrated on the champion device which was blade coated at a substrate temperature of 120°C in ambient conditions. Although these

FIGURE 6 | Formation of the mixed cation perovskite film in ambient conditions using the hot-substrate method **(A)** Illustration of the blade-coating method on the hot substrate at temperature between 100°C and 145°C. Illustration of the free energy of α-phase and α-phase at **(B)** room temperature and **(C)** at 145°C. Phase purity is illustrated and characterized by X-ray diffraction for **(D)** FAPbI$_3$ and **(E)** FA$_{0.4}$MA$_{0.6}$PbI$_3$, respectively, at different substrate temperatures. Reprinted with permission from Deng et al. (2016). Copyright 2016 WILEY-VCH Verlag GmbH & Co. KGaA, Weinheim.

triple cation CsFAMA–based PSCs exhibit a larger bandgap than MAPbI$_3$ PSCs, the blade-coated device performance still lags behind that of the MAPbI$_3$-based devices. Recently, Wu et al. successfully fabricated pure phase FA–dominated PSCs using the doctor blade–coating method, demonstrating a PCE over 22% (Wu et al., 2020). They found that a small amount of organic halide molecules, phenylethylammonium chloride (PEACl), could enhance the phase purity and stability of FA-alloyed PSCs. The PEACl molecules provided three functions for the enhanced nucleation and growth: 1) PEA$^+$ cations passivated the negatively charged A-site vacancies; 2) Cl$^-$ anions altered the nucleation and grain growth to achieve a compact and low defect density thin film; and 3) the hydrophobic conjugated rings provided a high moisture resistance to the perovskite precursor.

Apart from compositional engineering, solvent engineering also plays a key role in the ambient fabrication of perovskite thin films. Yang et al. (2017) developed an excess chlorine–containing MAPbI$_3$ precursor solution with proper solvent tuning and coupled with anti-solvent bathing, to increase the processing window up to 8 min and create a rapid grain growth, at room temperature with RH = 10–20%. The ink used for both spin coating and blade coating resulted in comparable film morphology and device performance. The improved film morphology was attributed to the Ostwald ripening of the grains (recrystallization of the perovskite film to form large grains during the annealing stage). A four-cell module (12.6 cm^2 with 88% geometric fill factor) was demonstrated with a stabilized efficiency of 13.3%.

Blade coating is a facile and roll-to-roll–compatible deposition method for manufacturing. It is scalable and reduces the wastage of material (compared to the spin-coating method). For manufacturing, it is also desired to achieve a high-throughput process. Hence, fast blading speed in air is necessary. Deng et al. reported the use of surfactant to enhance the wettability of the ink solution especially fabricated on the p–i–n structure using the hydrophobic PTTA hole transport layer (Deng et al., 2018). A fast blading speed of 180 m h^{-1} was achieved by adding 20 ppm surfactants into the ink solution. In addition, the surfactants passivated the traps which produced ambient blade–coated PSCs of PCE over 20%.

Gas-assisted drying has been demonstrated to remove solvent effectively such that the supersaturation condition is achieved, and nucleation is started in glovebox-processed PSCs (Huang et al., 2014; Deng et al., 2019; Green et al., 2019). Recently, our group reported highly efficient PSCs (PCE = 21.1%) fabricated at room temperature in ambient conditions of 55% RH by the meniscus blade–coating method using air-knife–assisted drying to accelerate the evaporation of solvent (Fong et al., 2021). *In situ* UV-Vis spectroscopy studies were conducted to quantitatively analyze the influence of blowing gas velocity on the nucleation rate in the solution-to-solid solidification process. A gas blowing velocity of 42 m s^{-1} enabled the fabrication of PSCs with steady PCE under ambient conditions up to 65% RH. Comparison of some representative PSCs with the perovskite thin films fabricated in the ambient environment are summarized in **Table 2**.

SUMMARY AND OUTLOOK

Remarkable progress in the stability and efficiency of perovskite solar cells has been demonstrated in laboratory small-scaled devices fabricated in an inert gas–filled glovebox. The blade-coating method is a promising technique which is compatible with the roll-to-roll manufacturing process. Extensive studies of solvent engineering, precursor composition engineering, adding additives, adding surfactants, hot-substrate coating, and gas-assisted drying on the nucleation of the perovskite by meniscus blade coating of perovskite thin films in ambient conditions have been conducted. Recently, fast blading speed has been reported attributed to the improved wettability by surfactant. Device stability has also been widely studied by controlling the nucleation process in the ambient environment. The most processing challenge falls into the game-changing parameter—ambient moisture. Extensive studies showed that water molecules could facilitate the formation of large grains but could also result in material degradation. More studies are needed in the future in compositional engineering not only due to the phase, thermal, and chemical stability but also due to the environmental impact. The photovoltaic performance of Pb-free perovskite PSCs lags behind that of the Pb-based PSCs. However, the toxicity of Pb and solvent would hinder the manufacturing process until a robust encapsulation process is well-developed. A recent computational study provided in-depth understanding and strategies to improving the stability of PSCs against moisture through compositional engineering (Li et al., 2021). More studies could be performed in this direction to achieve a Pb-free ambient air–processed PSC.

AUTHOR CONTRIBUTIONS

PF and GL conceived the idea. PF wrote the manuscript.

FUNDING

REFERENCES

Aranda, C., Cristobal, C., Shooshtari, L., Li, C., Huettner, S., and Guerrero, A. (2017). Formation criteria of high efficiency perovskite solar cells under ambient conditions. *Sustainable Energy Fuels* 1 (3), 540–547. doi:10.1039/c6se00077k

Ba, Q., Jana, A., Wang, L., and Kim, K. S. (2019). Dual emission of water-stable 2D organic–inorganic halide perovskites with Mn(II) dopant. *Adv. Funct. Mater.* 29 (43), 1904768. doi:10.1002/adfm.201904768

Bi, Z., Rodríguez-Martínez, X., Aranda, C., Pascual-San-José, E., Goñi, A. R., Campoy-Quiles, M., et al. (2018). Defect tolerant perovskite solar cells from blade coated non-toxic solvents. *J. Mater. Chem.* 6 (39), 19085–19093. doi:10.1039/c8ta06771f

Cheng, R., Chung, C. C., Zhang, H., Zhou, Z., Zhai, P., Huang, Y. T., et al. (2019). An air knife-assisted recrystallization method for ambient-process planar perovskite solar cells and its dim-light harvesting. *Small* 15 (8), e1804465. doi:10.1002/smll.201804465

Cheng, Y., Xu, X., Xie, Y., Li, H.-W., Qing, J., Ma, C., et al. (2017). 18% high-efficiency air-processed perovskite solar cells made in a humid atmosphere of 70% RH. *Solar RRL* 1 (9), 1700097. doi:10.1002/solr.201700097

Chiang, C.-H., Nazeeruddin, M. K., Grätzel, M., and Wu, C.-G. (2017). The synergistic effect of H_2O and DMF towards stable and 20% efficiency inverted perovskite solar cells. *Energy Environ. Sci.* 10 (3), 808–817. doi:10.1039/c6ee03586h

Contreras-Bernal, L., Aranda, C., Valles-Pelarda, M., Ngo, T. T., Ramos-Terrón, S., Gallardo, J. J., et al. (2018). Homeopathic perovskite solar cells: effect of humidity during fabrication on the performance and stability of the device. *J. Phys. Chem. C* 122 (10), 5341–5348. doi:10.1021/acs.jpcc.8b01558

Correa-Baena, J.-P., Saliba, M., Buonassisi, T., Grätzel, M., Abate, A., Tress, W., et al. (2017). Promises and challenges of perovskite solar cells. *Science* 358 (6364), 739–744. doi:10.1126/science.aam6323

Cui, X.-P., Jiang, K.-J., Huang, J.-H., Zhou, X.-Q., Su, M.-J., Li, S.-G., et al. (2015). Electrodeposition of PbO and its *in situ* conversion to $CH_3NH_3PbI_3$ for mesoscopic perovskite solar cells. *Chem. Commun.* 51 (8), 1457–1460. doi:10.1039/C4CC08269A

Dai, X. Z., Deng, Y. H., Van Brackle, C. H., Chen, S. S., Rudd, P. N., Xiao, X., et al. (2020). Scalable fabrication of efficient perovskite solar modules on flexible glass substrates. *Advanced Energy Materials* 10 (1), 1903108. doi:10.1002/aenm.201903108

Deng, Y. H., Dong, Q. F., Bi, C., Yuan, Y. B., and Huang, J. S. (2016). Air-stable, efficient mixed-cation perovskite solar cells with Cu electrode by scalable fabrication of active layer. *Advanced Energy Materials* 6 (11), 1600372. doi:10.1002/aenm.201600372

Deng, Y. H., Zheng, X. P., Bai, Y., Wang, Q., Zhao, J. J., and Huang, J. S. (2018). Surfactant-controlled ink drying enables high-speed deposition of perovskite films for efficient photovoltaic modules. *Nature Energy* 3 (7), 560–566. doi:10.1038/s41560-018-0153-9

Deng, Y., Peng, E., Shao, Y., Xiao, Z., Dong, Q., and Huang, J. (2015). Scalable fabrication of efficient organolead trihalide perovskite solar cells with doctor-bladed active layers. *Energy Environ. Sci.* 8 (5), 1544–1550. doi:10.1039/c4ee03907f

Deng, Y., Van Brackle, C. H., Dai, X., Zhao, J., Chen, B., and Huang, J. (2019). Tailoring solvent coordination for high-speed, room-temperature blading of perovskite photovoltaic films. *Sci Adv* 5 (12), eaax7537. doi:10.1126/sciadv.aax7537

Ding, J., Han, Q. W., Ge, Q. Q., Xue, D. J., Ma, J. Y., Zhao, B. Y., et al. (2019). Fully air-bladed high-efficiency perovskite photovoltaics. *Joule* 3 (2), 402–416. doi:10.1016/j.joule.2018.10.025

Dong, Q., Yuan, Y., Shao, Y., Fang, Y., Wang, Q., and Huang, J. (2015). Abnormal crystal growth in $CH_3NH_3PbI_{3-x}Cl_x$ using a multi-cycle solution coating process. *Energy Environ. Sci.* 8 (8), 2464–2470. doi:10.1039/c5ee01179e

Dunlap-Shohl, W. A., Zhou, Y., Padture, N. P., and Mitzi, D. B. (2019). Synthetic approaches for halide perovskite thin films. *Chem. Rev.* 119 (5), 3193–3295. doi:10.1021/acs.chemrev.8b00318

Fan, Y., Fang, J., Chang, X., Tang, M.-C., Barrit, D., Xu, Z., et al. (2019). Scalable ambient fabrication of high-performance $CsPbI_2Br$ solar cells. *Joule* 3 (10), 2485–2502. doi:10.1016/j.joule.2019.07.015

Fong, P. W. K., Hu, H., Ren, Z., Liu, K., Cui, L., Bi, T., et al. (2021). Printing high-efficiency perovskite solar cells in high-humidity ambient environment—an in-situ guided investigation. *Adv. Sci.* 8 (6). doi:10.1002/advs.202003359

Galagan, Y., Di Giacomo, F., Gorter, H., Kirchner, G., de Vries, I., Andriessen, R., et al. (2018). Roll-to-Roll slot die coated perovskite for efficient flexible solar cells. *Advanced Energy Materials* 8 (32), 1801935. doi:10.1002/aenm.201801935

Gao, H., Bao, C., Li, F., Yu, T., Yang, J., Zhu, W., et al. (2015). Nucleation and crystal growth of organic-inorganic lead halide perovskites under different

relative humidity. *ACS Appl. Mater. Interfaces* 7 (17), 9110–9117. doi:10.1021/acsami.5b00895

Gong, X., Li, M., Shi, X.-B., Ma, H., Wang, Z.-K., and Liao, L.-S. (2015). Controllable perovskite crystallization by water additive for high-performance solar cells. *Adv. Funct. Mater.* 25 (42), 6671–6678. doi:10.1002/adfm.201503559

Green, M. A., Dunlop, E. D., Levi, D. H., Hohl-Ebinger, J., Yoshita, M., and Ho-Baillie, A. W. Y. (2019). Solar cell efficiency tables (version 54). *Prog. Photovoltaics Res. Appl.* 27 (7), 565–575. doi:10.1002/pip.3171

He, M., Li, B., Cui, X., Jiang, B., He, Y., Chen, Y., et al. (2017). Meniscus-assisted solution printing of large-grained perovskite films for high-efficiency solar cells. *Nat. Commun.* 8, 16045. doi:10.1038/ncomms16045

Heo, J. H., Han, H. J., Kim, D., Ahn, T. K., and Im, S. H. (2015a). Hysteresis-less inverted CH₃NH₃PbI₃ planar perovskite hybrid solar cells with 18.1% power conversion efficiency. *Energy Environ. Sci.* 8 (5), 1602–1608. doi:10.1039/c5ee00120j

Heo, J. H., Song, D. H., Han, H. J., Kim, S. Y., Kim, J. H., Kim, D., et al. (2015b). Planar CH₃NH₃PbI₃ perovskite solar cells with constant 17.2% average power conversion efficiency irrespective of the scan rate. *Adv. Mater.* 27 (22), 3424–3430. doi:10.1002/adma.201500048

Heo, J. H., Lee, M. H., Jang, M. H., and Im, S. H. (2016). Highly efficient CH₃NH₃PbI₃₋ₓClₓ mixed halide perovskite solar cells prepared by re-dissolution and crystal grain growth via spray coating. *J. Mater. Chem.* 4 (45), 17636–17642. doi:10.1039/C6TA06718B

Heo, J. H., Song, D. H., and Im, S. H. (2014). Planar CH₃NH₃PbBr₃ hybrid solar cells with 10.4% power conversion efficiency, fabricated by controlled crystallization in the spin-coating process. *Adv. Mater.* 26 (48), 8179–8183. doi:10.1002/adma.201403140

Hu, H., Ren, Z., Fong, P. W. K., Qin, M., Liu, D., Lei, D., et al. (2019). Room-temperature meniscus coating of >20% perovskite solar cells: a film formation mechanism investigation. *Adv. Funct. Mater.* 29 (25), 1900092. doi:10.1002/adfm.201900092

Hu, H., Singh, M., Wan, X., Tang, J., Chu, C.-W., and Li, G. (2020). Nucleation and crystal growth control for scalable solution-processed organic–inorganic hybrid perovskite solar cells. *J. Mater. Chem.* 8 (4), 1578–1603. doi:10.1039/c9ta11245f

Huang, F., Dkhissi, Y., Huang, W., Xiao, M., Benesperi, I., Rubanov, S., et al. (2014). Gas-assisted preparation of lead iodide perovskite films consisting of a monolayer of single crystalline grains for high efficiency planar solar cells. *Nanomater. Energy* 10, 10–18. doi:10.1016/j.nanoen.2014.08.015

Huang, J.-h., Jiang, K.-j., Cui, X.-p., Zhang, Q.-q., Gao, M., Su, M.-j., et al. (2015). Direct conversion of CH₃NH₃PbI₃ from electrodeposited PbO for highly efficient planar perovskite solar cells. *Sci. Rep.* 5 (1), 15889. doi:10.1038/srep15889

Huang, S. H., Tian, K. Y., Huang, H. C., Li, C. F., Chu, W. C., Lee, K. M., et al. (2020). Controlling the morphology and interface of the perovskite layer for scalable high-efficiency solar cells fabricated using green solvents and blade coating in an ambient environment. *ACS Appl. Mater. Interfaces* 12 (23), 26041–26049. doi:10.1021/acsami.0c06211

Hwang, K., Jung, Y. S., Heo, Y. J., Scholes, F. H., Watkins, S. E., Subbiah, J., et al. (2015). Toward large scale roll-to-roll production of fully printed perovskite solar cells. *Adv. Mater.* 27 (7), 1241–1247. doi:10.1002/adma.201404598

Jana, A., and Kim, K. S. (2018). Water-stable, fluorescent Organic−Inorganic hybrid and fully inorganic perovskites. *Acs Energy Letters* 3 (9), 2120–2126. doi:10.1021/acsenergylett.8b01394

Jung, J. W., Williams, S. T., and Jen, A. K. Y. (2014). Low-temperature processed high-performance flexible perovskite solar cells via rationally optimized solvent washing treatments. *RSC Adv.* 4 (108), 62971–62977. doi:10.1039/c4ra13212b

Kim, H. S., Lee, C. R., Im, J. H., Lee, K. B., Moehl, T., Marchioro, A., et al. (2012). Lead iodide perovskite sensitized all-solid-state submicron thin film mesoscopic solar cell with efficiency exceeding 9%. *Sci. Rep.* 2, 591. doi:10.1038/srep00591

Kim, J. H., Williams, S. T., Cho, N., Chueh, C.-C., and Jen, A. K. Y. (2015). Enhanced environmental stability of planar heterojunction perovskite solar cells based on blade-coating. *Advanced Energy Materials* 5 (4), 1401229. doi:10.1002/aenm.201401229

Ko, H.-S., Lee, J.-W., and Park, N.-G. (2015). 15.76% efficiency perovskite solar cells prepared under high relative humidity: importance of PbI₂ morphology in two-step deposition of CH₃NH₃PbI₃. *J. Mater. Chem.* 3 (16), 8808–8815. doi:10.1039/c5ta00658a

Kojima, A., Teshima, K., Shirai, Y., and Miyasaka, T. (2009). Organometal halide perovskites as visible-light sensitizers for photovoltaic cells. *J. Am. Chem. Soc.* 131 (17), 6050–6051. doi:10.1021/ja809598r

Kong, W., Wang, G., Zheng, J., Hu, H., Chen, H., Li, Y., et al. (2018). Fabricating high-efficient blade-coated perovskite solar cells under ambient condition using lead acetate trihydrate. *Solar RRL* 2 (3), 1770153. doi:10.1002/solr.201700214

Lawrence, C. J. (1988). The mechanics of spin coating of polymer films. *Phys. Fluids* 31 (10), 2786. doi:10.1063/1.866986

Le Berre, M., Chen, Y., and Baigl, D. (2009). From convective assembly to Landau−Levich deposition of multilayered phospholipid films of controlled thickness. *Langmuir* 25 (5), 2554–2557. doi:10.1021/la803646e

Lee, M. M., Teuscher, J., Miyasaka, T., Murakami, T. N., and Snaith, H. J. (2012). Efficient hybrid solar cells based on meso-superstructured organometal halide perovskites. *Science* 338 (6107), 643–647. doi:10.1126/science.1228604

Leguy, A. M. A., Hu, Y., Campoy-Quiles, M., Alonso, M. I., Weber, O. J., Azarhoosh, P., et al. (2015). Reversible hydration of CH₃NH₃PbI₃in films, single crystals, and solar cells. *Chem. Mater.* 27 (9), 3397–3407. doi:10.1021/acs.chemmater.5b00660

Li, Q., Chen, Z., Tranca, I., Gaastra-Nedea, S., Smeulders, D., and Tao, S. (2021). Compositional effect on water adsorption on metal halide perovskites. *Appl. Surf. Sci.* 538, 148058. doi:10.1016/j.apsusc.2020.148058

Li, S.-G., Jiang, K.-J., Su, M.-J., Cui, X.-P., Huang, J.-H., Zhang, Q.-Q., et al. (2015). Inkjet printing of CH₃NH₃PbI₃ on a mesoscopic TiO₂ film for highly efficient perovskite solar cells. *J. Mater. Chem.* 3 (17), 9092–9097. doi:10.1039/C4TA05675B

Liu, C., Ding, W. H., Zhou, X. Y., Gao, J. S., Cheng, C., Zhao, X. Z., et al. (2017). Efficient and stable perovskite solar cells prepared in ambient air based on surface-modified perovskite layer. *J. Phys. Chem. C* 121 (12), 6546–6553. doi:10.1021/acs.jpcc.7b00847

Liu, K., Liang, Q., Qin, M., Shen, D., Yin, H., Ren, Z., et al. (2020). Zwitterionic-surfactant-assisted room-temperature coating of efficient perovskite solar cells. *Joule* 4, 2404–2425. doi:10.1016/j.joule.2020.09.011

Liu, M., Johnston, M. B., and Snaith, H. J. (2013). Efficient planar heterojunction perovskite solar cells by vapour deposition. *Nature* 501 (7467), 395–398. doi:10.1038/nature12509

Mallajosyula, A. T., Fernando, K., Bhatt, S., Singh, A., Alphenaar, B. W., Blancon, J.-C., et al. (2016). Large-area hysteresis-free perovskite solar cells via temperature controlled doctor blading under ambient environment. *Applied Materials Today* 3, 96–102. doi:10.1016/j.apmt.2016.03.002

Mei, A., Li, X., Liu, L., Ku, Z., Liu, T., Rong, Y., et al. (2014). A hole-conductor–free, fully printable mesoscopic perovskite solar cell with high stability. *Science* 345 (6194), 295–298. doi:10.1126/science.1254763

Noh, J. H., Im, S. H., Heo, J. H., Mandal, T. N., and Seok, S. I. (2013). Chemical management for colorful, efficient, and stable inorganic–organic hybrid nanostructured solar cells. *Nano Lett.* 13 (4), 1764–1769. doi:10.1021/nl400349b

NREL (2020). *Solar cell efficiency chart*. Available at: https://www.nrel.gov/pv/cell-efficiency.html (Accessed May, 2020).

Pathak, S., Sepe, A., Sadhanala, A., Deschler, F., Haghighirad, A., Sakai, N., et al. (2015). Atmospheric influence upon crystallization and electronic disorder and its impact on the photophysical properties of organic–inorganic perovskite solar cells. *ACS Nano* 9 (3), 2311–2320. doi:10.1021/nn506465n

Qin, T., Huang, W., Kim, J.-E., Vak, D., Forsyth, C., McNeill, C. R., et al. (2017). Amorphous hole-transporting layer in slot-die coated perovskite solar cells. *Nanomater. Energy* 31, 210–217. doi:10.1016/j.nanoen.2016.11.022

Radicchi, E., Ambrosio, F., Mosconi, E., Alasmari, A. A., Alasmary, F. A. S., and De Angelis, F. (2020). Combined computational and experimental investigation on the nature of hydrated iodoplumbate complexes: insights into the dual role of water in perovskite precursor solutions. *J. Phys. Chem. B* 124 (50), 11481–11490. doi:10.1021/acs.jpcb.0c08624

Rong, Y., Hou, X., Hu, Y., Mei, A., Liu, L., Wang, P., et al. (2017). Synergy of ammonium chloride and moisture on perovskite crystallization for efficient printable mesoscopic solar cells. *Nat. Commun.* 8, 14555. doi:10.1038/ncomms14555

Saliba, M., Matsui, T., Seo, J.-Y., Domanski, K., Correa-Baena, J.-P., Nazeeruddin, M. K., et al. (2016). Cesium-containing triple cation perovskite solar cells: improved stability, reproducibility and high efficiency. *Energy Environ. Sci.* 9 (6), 1989–1997. doi:10.1039/C5EE03874J

Seo, J., Park, S., Chan Kim, Y., Jeon, N. J., Noh, J. H., Yoon, S. C., et al. (2014). Benefits of very thin PCBM and LiF layers for solution-processed p–i–n perovskite solar cells. *Energy Environ. Sci.* 7 (8), 2642–2646. doi:10.1039/C4EE01216J

Singh, T., and Miyasaka, T. (2018). Stabilizing the efficiency beyond 20% with a mixed cation perovskite solar cell fabricated in ambient air under controlled humidity. *Advanced Energy Materials* 8 (3), 1700677. doi:10.1002/aenm.201700677

Tai, Q., You, P., Sang, H., Liu, Z., Hu, C., Chan, H. L., et al. (2016). Efficient and stable perovskite solar cells prepared in ambient air irrespective of the humidity. *Nat. Commun.* 7, 11105. doi:10.1038/ncomms11105

Tait, J. G., Manghooli, S., Qiu, W., Rakocevic, L., Kootstra, L., Jaysankar, M., et al. (2016). Rapid composition screening for perovskite photovoltaics via concurrently pumped ultrasonic spray coating. *J. Mater. Chem.* 4 (10), 3792–3797. doi:10.1039/C6TA00739B

Tang, M.-C., Fan, Y., Barrit, D., Chang, X., Dang, H. X., Li, R., et al. (2020). Ambient blade coating of mixed cation, mixed halide perovskites without dripping: *in situ* investigation and highly efficient solar cells. *J. Mater. Chem.* 8 (3), 1095–1104. doi:10.1039/c9ta12890e

Tang, S., Deng, Y. H., Zheng, X. P., Bai, Y., Fang, Y. J., Dong, Q. F., et al. (2017). Composition engineering in doctor-blading of perovskite solar cells. *Advanced Energy Materials* 7 (18), 1700302. doi:10.1002/aenm.201700302

Ternes, S., Bornhorst, T., Schwenzer, J. A., Hossain, I. M., Abzieher, T., Mehlmann, W., et al. (2019). Drying dynamics of solution-processed perovskite thin-film photovoltaics: in situ characterization, modeling, and process control. *Advanced Energy Materials* 9 (39), 1901581. doi:10.1002/aenm.201901581

Thanh, N. T. K., Maclean, N., and Mahiddine, S. (2014). Mechanisms of nucleation and growth of nanoparticles in solution. *Chem. Rev.* 114 (15), 7610–7630. doi:10.1021/cr400544s

Troughton, J., Hooper, K., and Watson, T. M. (2017). Humidity resistant fabrication of $CH_3NH_3PbI_3$ perovskite solar cells and modules. *Nano Energy* 39, 60–68. doi:10.1016/j.nanoen.2017.06.039

van Hardeveld, R. M., Gunter, P. L. J., van Ijzendoorn, L. J., Wieldraaijer, W., Kuipers, E. W., and Niemantsverdriet, J. W. (1995). Deposition of inorganic salts from solution on flat substrates by spin-coating: theory, quantification and application to model catalysts. *Appl. Surf. Sci.* 84 (4), 339–346. doi:10.1016/0169-4332(95)00010-0

Wang, W.-T., Sharma, J., Chen, J.-W., Kao, C.-H., Chen, S.-Y., Chen, C.-H., et al. (2018). Nanoparticle-induced fast nucleation of pinhole-free PbI_2 film for ambient-processed highly-efficient perovskite solar cell. *Nanomater. Energy* 49, 109–116. doi:10.1016/j.nanoen.2018.03.081

Wu, C.-G., Chiang, C.-H., Tseng, Z.-L., Nazeeruddin, M. K., Hagfeldt, A., and Grätzel, M. (2015). High efficiency stable inverted perovskite solar cells without current hysteresis. *Energy Environ. Sci.* 8 (9), 2725–2733. doi:10.1039/c5ee00645g

Wu, W. Q., Rudd, P. N., Wang, Q., Yang, Z., and Huang, J. (2020). Blading phase-pure formamidinium-alloyed perovskites for high-efficiency solar cells with low photovoltage deficit and improved stability. *Adv. Mater.* 32 (28), 2000995. doi:10.1002/adma.202000995

Wu, W. Q., Wang, Q., Fang, Y., Shao, Y., Tang, S., Deng, Y., et al. (2018). Molecular doping enabled scalable blading of efficient hole-transport-layer-free perovskite solar cells. *Nat. Commun.* 9 (1), 1625. doi:10.1038/s41467-018-04028-8

Yang, M. J., Li, Z., Reese, M. O., Reid, O. G., Kim, D. H., Siol, S., et al. (2017). Perovskite ink with wide processing window for scalable high-efficiency solar cells. *Nature Energy* 2 (5), 17038. doi:10.1038/nenergy.2017.38

Yang, Z., Chueh, C.-C., Zuo, F., Kim, J. H., Liang, P.-W., and Jen, A. K. Y. (2015). High-performance fully printable perovskite solar cells via blade-coating technique under the ambient condition. *Advanced Energy Materials* 5 (13), 1500328. doi:10.1002/aenm.201500328

You, J., Yang, Y., Hong, Z., Song, T.-B., Meng, L., Liu, Y., et al. (2014). Moisture assisted perovskite film growth for high performance solar cells. *Appl. Phys. Lett.* 105 (18), 183902. doi:10.1063/1.4901510

Zhong, Y. F., Munir, R., Li, J. B., Tang, M. C., Niazi, M. R., Smilgies, D. M., et al. (2018). Blade-coated hybrid perovskite solar cells with efficiency > 17%: an in situ investigation. *ACS Energy Letters* 3 (5), 1078–1085. doi:10.1021/acsenergylett.8b00428

Zhou, H., Chen, Q., Li, G., Luo, S., Song, T.-b., Duan, H.-S., et al. (2014). Interface engineering of highly efficient perovskite solar cells. *Science* 345 (6196), 542–546. doi:10.1126/science.1254050